

Multiparticle tunnelling in diffusive superconducting junctions

E V Bezuglyi^{†‡}, A S Vasenko^{†§}, E N Bratus'[‡], V S Shumeiko[†] and G Wendin[†]

[†] Chalmers University of Technology, S-41296 Göteborg, Sweden

[‡] B Verkin Institute for Low Temperature Physics and Engineering, Kharkov 61103, Ukraine

[§] Department of Physics, Moscow State University, Moscow 119992, Russia

E-mail: eugene.bezuglyi@gmail.com

Abstract. We formulate a theoretical framework to describe multiparticle current transport in planar superconducting tunnel junctions with diffusive electrodes. The approach is based on direct solving of quasiclassical Keldysh-Green function equations for nonequilibrium superconductors, and consists of a combination of a circuit theory analysis and improved perturbation expansion. The theory predicts much greater scaling parameter for the subharmonic gap structure of the tunnel current in diffusive junctions compared to the one in ballistic junctions and mesoscopic constrictions with the same barrier transparency.

PACS numbers: 74.45.+c, 74.40.+k, 74.25.Fy, 74.50.+r.

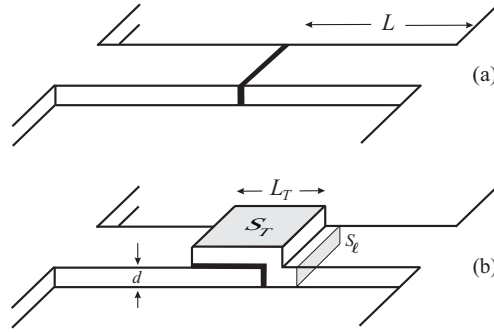


Figure 1. One-dimensional (a) and planar (b) models of the tunnel junction.

1. Introduction

Multiparticle tunnelling (MPT) is known to be a mechanism of dissipative current transport in superconducting tunnel junctions at the subgap applied voltage $eV < 2\Delta$, and at small temperature $T \ll \Delta$ [1]. It has been shown in [2, 3] that the MPT is completely equivalent to the *coherent* multiple Andreev reflection mechanism (MAR) [4, 5]. Here we use the term MPT to emphasize the low transparency, tunnel junction limit, leaving the term MAR for a general case of transparent weak links. Each MPT event can be considered as a chain of multiple Andreev reflections [6] accompanied by the transfer of n electrons through the tunnel barrier and eventually results in the creation of two quasiparticles which contribute to the dissipative current. This process manifests itself in the set of the current steps at $eV = 2\Delta/n$ – the subharmonic gap structure (SGS) – which is commonly observed in planar junctions with tunnel barriers [7, 8, 9, 10], and in tunable mesoscopic constrictions in the tunnelling regime [11, 12, 13]. The theory predicts the scaling $\approx D/2$ between the neighboring current steps in the tunnelling SGS, where D is the bare transparency of the junction tunnel barrier [1, 2, 3, 4]. However, in the experiment, the SGS scaling parameter is generally much larger. A common explanation for this enhancement is the imperfection of the junction insulating layer [6, 8, 14]. In our previous paper [15] the attention was drawn to an alternative explanation: effect of disorder in planar junction electrodes; it was predicted that the SGS scaling parameter for planar diffusive junctions is enhanced by a factor $\sim \xi_0/\ell$, or even $\sim \xi_0^2/\ell d$ depending on the junction geometry (ξ_0 is the coherence length, ℓ is the elastic mean free path, d is the thickness of electrodes).

In this paper we present a detailed theory of the MPT in planar Josephson tunnel junctions with diffusive thin-film electrodes and extensively discuss the details of the behaviour of the MPT currents and the relevant asymptotical methods. The theory is based on the direct solving of the diffusive equations of nonequilibrium superconductivity [16]. The main difficulty with this approach is related to essentially nonstationary character of the Josephson tunnel transport. While analytical and numerical methods are well developed for solving stationary Usadel equation [17] and nonequilibrium Keldysh-Usadel equation [18], the nonstationary problem was so far studied only numerically [19]. The central model assumption made in this paper and relevant for the tunnel regime concerns discrimination of nonzero harmonics of the Green's functions and the distribution function. This approximation turns the originally difficult problem into an analytically tractable one, and at the same time it captures all qualitative, and to large extent quantitative properties of the tunnelling SGS. Within this approximation we are able to develop a relatively simple and physically appealing calculation scheme, which combines the improved iterative procedure for evaluating the tunnelling density of states (DOS), and the circuit theory methods [18, 20] for evaluating the dc current.

The resulting physical picture of the MPT is as follows: The tunnelling processes create the local nonzero DOS inside the bulk energy gap in the vicinity of the tunnel junction. This allows quasiparticles to overcome the energy gap at a small applied voltage in several steps, by repeated bouncing between the junction electrodes (MAR). The spectral current through the energy gap, which determines the net charge current, is calculated by considering an effective circuit theory network representing the tunnelling process.

The effect of substantial enhancement of the SGS scaling factor can be qualitatively understood from a mesoscopic picture of the diffusive tunnelling transport, namely, tunnelling through a set of independent quasi-ballistic conducting channels with randomly distributed transparencies [20, 21]. Within this picture, the contribution of each channel can be evaluated using the ballistic MAR theory [2, 3, 4]. In constrictions with length $L \gg \ell$ the transparencies are spread over the interval $\sim (L/\ell)D \gg D$ [22], which implies that the junction transparency, and hence the SGS scaling factor, are effectively enhanced by the factor L/ℓ . This explanation, however, is valid only for short constrictions, $L \ll \xi_0$, while it does not apply to planar tunnel junctions with overlapping thin-film electrodes commonly used in experiments and shown in figure 1. In these structures, massive

pads (reservoirs) are fairly far from the junction ($L \gg \xi_0$); in such a situation the effective junction length is defined by the scale of spatial variation of the Green's function, i.e., by the coherence length. If the size L_T of the overlapping parts of the electrodes is comparable to the electrode thickness d , then the junction can be considered as an effectively one-dimensional (1D) one (see figure 1(a)); in this case, the SGS enhancement factor becomes ξ_0/ℓ . If the junction cross-section is much larger than the cross-section of the electrodes (see figure 1(b)), the current concentrates not at the junction but rather in electrodes [23], and an additional enhancement factor ξ_0/d appears in the SGS scaling, which coincides with the result of rigorous calculation in this paper. Remarkably, this enhancement concerns only the multiparticle currents, while the single-particle current is not affected and is proportional to the bare transparency D [24].

The paper is organized as follows. In its major part we develop a theory for the 1D junctions, figure 1(a), and discuss the extension to the planar junctions, figure 1(b), towards the end, in section 4. We start with discussion of basic equations and adopted approximations in section 2. Then we construct the circuit theory in section 3, and develop a perturbation theory for the DOS in section 5. The MPT currents are calculated in sections 6 and 7; the latter section includes also the calculation of the excess current. The effect of neglected harmonics in the Keldysh and Green's functions is evaluated in section 8. In section 9 we discuss the results and possible implications of the theory.

2. 1D junction model

2.1. Basic equations

The model of tunnel junction we are first going to study is depicted in figure 1(a) and consists of a tunnel barrier with the transparency D attached to bulk superconducting electrodes via two superconducting leads ($-L < x < 0$ and $0 < x < L$). We will consider a diffusive limit, in which the elastic scattering length ℓ is much smaller than the coherence length $\xi_0 = \sqrt{\mathcal{D}/2\Delta}$, where \mathcal{D} is the diffusion coefficient (we assume $\hbar = k_B = 1$). We assume the length L of the leads to be much larger than ξ_0 , and their width to be much smaller than the Josephson penetration depth which implies homogeneity of the current along the junction. Similar model has been considered in [25] in study of the dc Josephson effect in tunnel structures.

Under these conditions, the microscopic calculation of the electric current $I(t)$ requires solution of the diffusive equations of nonequilibrium superconductivity [16] for the 4×4 matrix two-time Keldysh-Green's function $\check{G}(x, t_1, t_2)$ in the leads,

$$\begin{aligned} [\check{H}, \circ\check{G}] &= i\mathcal{D}\partial_x\check{J}, & \check{J} &= \check{G} \circ \partial_x\check{G}, & \check{G} \circ \check{G} &= \delta(t_1 - t_2), \\ \check{H} &= [i\sigma_z\partial_t - e\varphi + \hat{\Delta}(t_1)]\delta(t_1 - t_2), & \hat{\Delta} &= e^{i\sigma_z\phi}i\sigma_y\Delta, \end{aligned} \quad (1)$$

where φ is the electric potential, Δ and ϕ are the modulus and the phase of the order parameter, respectively, σ_i are the Pauli matrices, ∂_x denotes partial derivative over the variable x and

$$\check{G} = \begin{pmatrix} \hat{g}^R & \hat{G}^K \\ 0 & \hat{g}^A \end{pmatrix}, \quad \hat{G}^K = \hat{g}^R \circ \hat{f} - \hat{f} \circ \hat{g}^A. \quad (2)$$

Here $\hat{g}^{R,A}$ are the 2×2 Nambu matrix retarded and advanced Green's functions, and $\hat{f} = f + \sigma_z f_-$ is the matrix distribution function (we use 'check' for 4×4 and 'hat' for 2×2 matrices). The multiplication procedure in (1) and (2) involves the time convolution

$$(A \circ B)(t_1, t_2) = \int_{-\infty}^{+\infty} A(t_1, t)B(t, t_2)dt. \quad (3)$$

For arbitrary tunnel barrier, the function \check{G} and the matrix current \check{J} at the left ($x = -0$) and the right ($x = +0$) sides of the tunnel junction are connected via the generalized boundary condition by Nazarov [20],

$$\check{J}_{-0} = \check{J}_{+0} = \frac{1}{2g_N R} \int_0^1 \frac{D\rho(D) dD [\check{G}_{-0}, \circ\check{G}_{+0}]}{1 + \frac{D}{4} \{\check{G}_{-0}, \circ\check{G}_{+0}\}}, \quad (4)$$

where $\rho(D)$ is the distribution of the transparencies of the conducting channels of the barrier ($\int_0^1 D\rho(D) dD = 1$), R is the junction resistance and g_N is the normal conductivity of the leads per unit length. Assuming the absence of high-transparent channels with $D \sim 1$ and considering $\rho(D)$ to be localized around the small value of $D \ll 1$ (tunnel limit), we can neglect the anti-commutator term in (4), thus arriving to the Kupriyanov-Lukichev's boundary condition [26],

$$\check{J}_{-0} = \check{J}_{+0} = (2g_N R)^{-1} [\check{G}_{-0}, \circ\check{G}_{+0}]. \quad (5)$$

The electric current is related to the Keldysh component of the matrix current \check{J} as $I(t) = (\pi g_N/4e) \text{Tr} \sigma_z \check{J}^K(x, t, t)$, and thus it can be expressed through the boundary value \check{J}_0 ,

$$I(t) = (\pi/8eR) \text{Tr} \sigma_z [\check{G}_{-0}, \circ \check{G}_{+0}]^K(t, t). \quad (6)$$

Equations (1) can be decomposed into the diffusion equations for the Green's functions,

$$[\hat{H}, \circ \hat{g}] = i\mathcal{D} \partial_x \hat{J}, \quad \hat{J} = \hat{g} \circ \partial_x \hat{g}, \quad \hat{g} \circ \hat{g} = \delta(t_1 - t_2), \quad (7)$$

and the equation for the Keldysh component \hat{G}^K ,

$$[\hat{H}, \circ \hat{G}^K] = i\mathcal{D} \partial_x \hat{J}^K, \quad \hat{J}^K = \hat{g}^R \circ \partial_x \hat{G}^K + \hat{G}^K \circ \partial_x \hat{g}^A, \quad (8a)$$

$$\hat{g}^R \circ \hat{G}^K + \hat{G}^K \circ \hat{g}^A = 0. \quad (8b)$$

The boundary conditions for the functions \hat{g} and \hat{G}^K at the tunnel barrier follow from (5),

$$\hat{J}_0 = (W/\xi_0) [\hat{g}_{-0}, \circ \hat{g}_{+0}], \quad (9a)$$

$$\hat{J}_0^K = (W/\xi_0) [\check{G}_{-0}, \circ \check{G}_{+0}]^K. \quad (9b)$$

In (9a) and (9b), the transparency parameter W is defined as

$$W = R(\xi_0)/2R = (3\xi_0/4\ell)D \gg D, \quad (10)$$

where $R(\xi_0) = \xi_0/g_N$ is the normal resistance of the piece of the lead with the length ξ_0 . It has been shown in [25] that it is the parameter W rather than the barrier transparency D that plays the role of a true transparency parameter in diffusive tunnel junctions. We will consider the limit $W \ll 1$, which corresponds to the conventional tunnelling concept. In this case, according to (9a) and (9b), the gradients of all functions are small. Within the tunnel model, which assumes W to be the smallest parameter in the theory, these gradients are neglected, and the functions \hat{g} and \hat{f} are taken local-equilibrium within the leads. In our consideration, we will lift this assumption and suppose the local-equilibrium form of these functions only within the bulk electrodes (reservoirs). Attributing the reference point for the phase, $\phi = 0$, to the left electrode, $x = -L$, these functions in the right electrode, $x = L$, are given by relations

$$\hat{g}(E, t) = \sigma_z u(E + \sigma_z eV) + i e^{i\sigma_z \phi(t)} \sigma_y v(E), \quad (11a)$$

$$(u, v) = (E, \Delta)/\xi, \quad \xi^{R,A} = [(E \pm i0)^2 - \Delta^2]^{1/2}, \quad (11b)$$

$$\hat{f}(E) = \tanh[(E + \sigma_z eV)/2T], \quad (11c)$$

written in terms of the mixed Wigner representation $A(E, t)$ of the two-time functions,

$$A(t_1, t_2) = \int_{-\infty}^{+\infty} \frac{dE}{2\pi} e^{-iE(t_1 - t_2)} A(E, t),$$

where the variable E has the meaning of the quasiparticle energy, and $t = (t_1 + t_2)/2$ is a real time. Similar equations, with $\phi = 0$ and $V = 0$, apply to the left electrode, $x = -L$.

Because of the small value of the tunnelling parameter W one can neglect variations of the superconducting phase along the leads, as well as the charge imbalance function f_- proportional to a small electric field penetrating the superconducting leads. Furthermore, the small value of the superfluid momentum in the superconducting leads, $p_s \sim W$ [25], allows us to neglect a small effect of the energy gap suppression by the superfluid momentum ($\sim p_s^{4/3} \sim W^{4/3}$ [27]). Within such an approximation, the coefficients in (1) at the left lead, $x < 0$, are time-independent functions. At $x > 0$, applying the gauge transformation [28] $\check{G}(t_1, t_2) = S^\dagger(t_1) \check{G}(t_1, t_2) S(t_2)$ with a unitary operator $S(t) = \exp[i\sigma_z \phi(t)/2]$ to the function \check{G} , we exclude the time-dependent phase and the electric potential from the equations for the function \check{G} and corresponding boundary conditions at $x = L$, which then become similar to the equations for $\check{G}(x)$ at $x < 0$ and the boundary conditions at $x = -L$. This results in the symmetry relation $\check{G}(x) = \check{G}(-x)$, which allows us to replace the function \check{G}_{+0} in the boundary condition (5) and in the expression (6) for the electric current by the inverse gauge transformation of the function \check{G}_{-0} , $\check{G}_{+0} \rightarrow \check{G}_{-0} \equiv S(t_1) \check{G}_{+0} S^\dagger(t_2) = S(t_1) \check{G}_{-0} S^\dagger(t_2)$.

As the result, the problem is reduced to the solution of a static equation within the left lead for the function $\check{G}(x, t_1, t_2)$, completed with the time-dependent boundary condition (5) at the tunnel barrier. Similar approach is used in the theory of ballistic point contacts [2] where the Josephson coupling is described by an effective time-dependent matching condition for the gauge-transformed Bogolyubov-de Gennes equations in the leads.

It is convenient to expand all functions over harmonics of the Josephson frequency, $A(E, t) = \sum_m A(E, m) \exp(-2ieVmt)$, using the following rules for representation of the products and gauge-transformed values,

$$(A \circ B)(E, m) = \sum_{m'} A[E + eV(m - m'), m'] B(E - eVm', m - m'), \quad (12)$$

$$\bar{\hat{A}}(E, m) = \begin{pmatrix} A_{11}(E + eV, m), & A_{12}(E, m + 1) \\ A_{21}(E, m - 1), & A_{22}(E - eV, m) \end{pmatrix}. \quad (13)$$

In such a representation, the expression (6) for the dc current I has the following form

$$\begin{aligned} I &= \int_{-\infty}^{\infty} \frac{dE}{16eR} \text{Tr}(\hat{h} \circ \bar{\hat{G}}^{\text{K}} - \bar{\hat{h}} \circ \hat{G}^{\text{K}})(E, 0) \\ &= \int_{-\infty}^{\infty} \frac{dE}{16eR} \text{Tr} \sum_m [\hat{h}(E, m) \bar{\hat{G}}^{\text{K}}(E, -m) \\ &\quad - \bar{\hat{h}}(E, m) \hat{G}^{\text{K}}(E, -m)], \quad \hat{h} = \sigma_z \hat{g}^{\text{R}} - \hat{g}^{\text{A}} \sigma_z, \end{aligned} \quad (14)$$

where all functions are taken at the boundary $x = -0$. We will adopt the same convention in the most of following equations and assume the spatial coordinate to be taken at the boundary.

2.2. Zero-harmonic model

Solving a system of nonlinear differential equations (7)–(9b) generally can be fulfilled only numerically even in the 1D case. The analytical solutions can be constructed in the adiabatic limit of small applied voltage $eV \ll \Delta$ [29]. To make the problem tractable at larger voltages $eV \sim \Delta$, we make use of the observation that the amplitudes of high-order harmonics of the function \hat{G} are small in the tunnelling limit $W \ll 1$: the amplitude of the m th harmonic decreases with m as W^m . This suggests that zero harmonics $m = 0$ play the key role in (14), while the high-order harmonics are neglected. Thus we adopt an approximation scheme, in which only the zero harmonics of the functions \hat{g} and \hat{G}^{K} are kept. It turns out that such an approximation is sufficiently powerful to recover all specific features of the MPT currents, and to give satisfactory description of the SGS of the net tunnel current. Furthermore, our analysis of the correction due to the first harmonics in section 8 shows that the zero-harmonic model may give rather good quantitative agreement with the result of full numerical calculation.

For the matrix structure of the zero harmonic of the function \hat{g} in (14), we adopt the form

$$\hat{g}(E, 0) = \sigma_z u(E) + i\sigma_y v(E), \quad u^2 - v^2 = 1, \quad (15)$$

which is similar to the Green's function structure (11a) in the left electrode, though u and v differ from their equilibrium values in (11b). It is possible to prove, using the normalization condition in (7), that the zero harmonic of matrix \hat{g} is traceless, and its σ_x -component is much smaller (at least by W^2) than the “main” components u and v , which have zero order in the parameter W . Within the same approximation, the Keldysh function has the form $\hat{G}^{\text{K}}(E, 0) = 2f(\sigma_z N + i\sigma_y M)$, where $N(E) = \text{Re} u^{\text{R}}$ is the density of states (DOS) normalized to its value in the normal state and $M(E) = \text{Re} v^{\text{R}}$. In what follows, we will express the advanced functions through the retarded ones, $(u, v)^{\text{A}} = -(u, v)^{\text{R}*}$, using the relation $\hat{g}^{\text{A}} = -\sigma_z \hat{g}^{\text{R}\dagger} \sigma_z$, and omit the superscript R, assuming all Green's functions to be retarded.

Retaining only zero harmonics of the functions \hat{g} and \hat{G}^{K} in (14), we find that only the diagonal parts $h(E)$ and $G^{\text{K}}(E)$ of the corresponding matrices enter the dc current

$$\begin{aligned} I &= \int_{-\infty}^{\infty} \frac{dE}{32eR} \text{Tr} \sum_{k=\pm 1} (1 + k\sigma_z) [h(E) G^{\text{K}}(E + keV) \\ &\quad - h(E + keV) G^{\text{K}}(E)]. \end{aligned} \quad (16)$$

By introducing the distribution function $n = \frac{1}{2}(1 - f)$ which approaches the Fermi function n_{F} in equilibrium, equation (16) exactly transforms to the standard form for the tunnel current,

$$I = \int_{-\infty}^{\infty} \frac{dE}{eR} N(E) N(E - eV) [n(E - eV) - n(E)], \quad (17)$$

with that essential difference that the DOS and the distribution function are not given, but are to be computed from the Keldysh-Green's function equations. To zero order in the tunnelling parameter, the DOS has the BCS form $N_{\text{S}}(E) = \text{Re}(E/\xi)$, and the distribution function is the equilibrium one, $n = n_{\text{F}}$. In this approximation, equation

(17) recovers the single-particle current of the tunnel model [24]. At zero temperature this current acquires the form

$$I = \int_{\Delta}^{eV-\Delta} \frac{dE}{eR} N_S(E) N_S(E - eV) \quad (18)$$

and turns to zero at $eV < 2\Delta$, having a sharp onset at $eV = 2\Delta$, $I_1(2\Delta) = \pi\Delta/2eR$.

To calculate the current at smaller, subgap voltages $eV < 2\Delta$, one has to calculate the tunnelling corrections to the BCS DOS, and to find the nonequilibrium distribution function.

3. Circuit representation of boundary condition

We start with evaluation of the distribution function and develop a circuit theory approach to derive a general analytical equation for the current (17) assuming the DOS to be modified in a close vicinity of the tunnel barrier.

3.1. Kinetic equation and boundary condition

Using zero harmonic of (8a) and (9b), we obtain the diffusive kinetic equation and the boundary condition,

$$\partial_x(D_+ \partial_x n) = 0, \quad (19)$$

$$D_+ \partial_x n|_{x=0} = (2W/\xi_0) \sum_{k=\pm 1} NN_k (n_k - n)|_{x=0}, \quad (20)$$

where $D_+ = \frac{1}{2}(1 + |u|^2 - |v|^2)$ is the dimensionless diffusion coefficient, and the subscript k denotes the energy shift: $n_k(E) \equiv n(E_k) = n(E + keV)$. It follows from (19) that $D_+ \partial_x n = \text{const}$; this constant value can be found from (20). At $x \gg \xi_0$ the coefficient D_+ approaches the BCS form $D_S = \Theta(|E| - \Delta)$ ($\Theta(x)$ is the Heaviside step function) and exactly turns to D_S at the reservoir, $x = -L$. This implies that at subgap energies $|E| < \Delta$, the quasiparticle probability current $D_+ \partial_x n$ turns to zero along the whole lead, and the distribution function is spatially homogeneous. Physically, this manifests complete Andreev reflection in terms of quasiparticle flows in diffusive structures.

Outside the gap, equation (19) has no bound solutions: the distribution function grows linearly with x far from the junction. Such a growth is limited in practice by inelastic collisions, which provide relaxation of $n(x, E)$ to the equilibrium value n_F at the distance of inelastic scattering length l_ε . To simplify the problem, we consider, instead of including a complicated inelastic collision term, a junction geometry with short enough leads having the length $L \ll l_\varepsilon$ (but still $L \gg \xi_0$) and connected at $x = \pm L$ to equilibrium reservoirs. Within this model, the Green's functions, which change at $x \sim \xi_0$, are not affected by the finite length of the leads, while the reservoirs impose the equilibrium boundary conditions for the distribution function, $n(\pm L) = n_F$. At the same time we can neglect inelastic collisions inside the leads. Obviously, this model describes a qualitative pattern of inelastic relaxation in very long channel ($L \gg l_\varepsilon$) with substitution $L \rightarrow l_\varepsilon$ in our results.

Generally, spatial variation of $n(x)$ at $|E| > \Delta$ has two scales: linear x -dependence at $x \sim L$ and fast but small variations near the junction due to spatial dependence of the Green's function. Neglecting these variations within the main approximation in the parameters W and ξ_0/L , we arrive at the relation $D_+ \partial_x n = [n(0) - n_F]L^{-1}$. Substituting it into the boundary condition (20) and accounting for $D_+ \partial_x n = 0$ at $|E| < \Delta$, we obtain the equation

$$\Theta(|E| - \Delta)(n - n_F) = r \sum_{k=\pm 1} NN_k (n_k - n). \quad (21)$$

In this and following equations, the functions are taken at the boundary $x = -0$. Equation (21) represents a recurrence relation between the values of $n(E)$ at the energies shifted by eV ; the nonequilibrium parameter r is defined as

$$r = 2LW/\xi_0 = R_N/R, \quad (22)$$

where $R_N = L/g_N$ is the normal resistance of one lead. In practice, the tunnel resistance much exceeds R_N , and the nonequilibrium parameter is small, $r \ll 1$, which implies that at the energies $|E| > \Delta$, the distribution function is always close to the Fermi function.

3.2. Circuit theory

We split the integral in (17) into pieces of length eV ,

$$I = \int_{-\infty}^{\infty} \frac{dE}{eR} j_0(E) = \int_0^{eV} \frac{dE}{eR} J(E), \quad (23)$$

$$J = \sum_{k=-\infty}^{\infty} j_k, \quad j_k = (n_{k-1} - n_k) \rho_k^{-1}, \quad \rho_k^{-1} = N_k N_{k-1}.$$

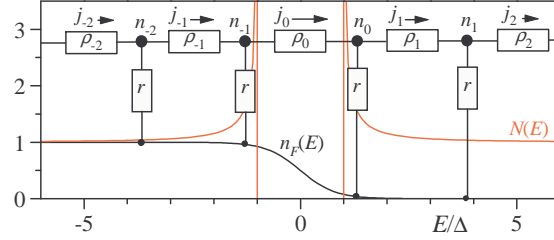


Figure 2. Circuit theory network with the period eV representing charge transport in diffusive tunnel junctions, $eV = 2.5\Delta$.

In these notations the recurrence relation (21) reads

$$\Theta(|E_k| - \Delta) [n_k - n_F(E_k)] = r(j_k - j_{k+1}). \quad (24)$$

A convenient interpretation of equations (23) and (24) in terms of the circuit theory [18] is given by an infinite network in the energy space with the period eV , graphically presented in figure 2. The electric current spectral density $J(E)$ consists of partial currents j_k which flow through the chain of tunnel “resistors” ρ_k connected to adjacent nodes of the network having “potentials” n_k and n_{k-1} . At $|E| > \Delta$, the nodes are also attached to the distributed “equilibrium source” $n_F(E)$ through equal resistors r . In this representation the recurrence relation (24) has the meaning of “Kirchhoff rules” for partial currents.

Below we assume the equilibrium quasiparticle distribution $n(E) = n_F(E)$ at $|E| > \Delta$, neglecting effect of small resistors r . In this limit, the currents j_k outside the energy gap, $|E_k| > \Delta$, vanish at zero temperature since n_F is piecewise constant. At $T \neq 0$, these currents describe the effect of thermal excitations. The subgap spectral current is conserved, $j_k = j_\Delta = \text{const}$, $k = 1 - N_-, \dots, N_+$ (as a consequence of (24)), and can be easily computed,

$$j_\Delta = [n_F(E_{-N_-}) - n_F(E_{N_+})] \rho_\Delta^{-1},$$

$$N_\pm(E) = \text{Int}[(\Delta \mp E)/eV] + 1, \quad \rho_\Delta(E) = \sum_{k=1-N_-}^{N_+} \rho_k,$$

where the integers $\pm N_\pm$ are the numbers of the nodes outside the gap nearest to the gap edges, $\text{Int}(x)$ denotes integer part of x , and the quantity $\rho_\Delta(E)$ has the meaning of the net subgap resistance. The subgap distribution function reads

$$n(E) = n_F(E_{N_+}) + [n_F(E_{-N_-}) - n_F(E_{N_+})] \sum_{k=1}^{N_+} \rho_k \rho_\Delta^{-1}. \quad (25)$$

The resulting electric current can be now written in a general form,

$$I = \int_0^{eV} \frac{dE}{eR} (N_- + N_+) j_\Delta + 2 \int_\Delta^\infty \frac{dE}{eR} \frac{n_F(E) - n_F(E_1)}{\rho_1}, \quad (26)$$

valid for arbitrary voltages and temperatures. Here the first term describes the subgap current, and the second term – the current of thermal excitations.

The magnitude of the subgap current is fully determined by the net subgap resistance; the current is blocked when this resistance is infinite, $\rho_\Delta = \infty$, which happens when DOS turns to zero. According to (26), the amount $N_- + N_+$ of the resistors contributing to the subgap resistance gives the amount of electric charge (in units of e) transferred during the tunnelling event. Thus, the circuit with one subgap resistor represents the single-particle tunnelling, which can exist only at $eV > 2\Delta$; in this case, equation (26) reduces to (18). At $eV < 2\Delta$, the subgap circuit should consist of at least two resistors (two-particle tunnelling). However, for the BCS DOS this current is blocked, and to evaluate the current one has to calculate the tunnelling correction to the DOS within the gap by solving the Green’s function equations.

4. Planar junctions

In this section we will discuss the extension of our approach to a more practical case of planar tunnel junction sketched in figure 1(b). This 2D case is more complex; however, it is possible to reduce this problem to the 1D case by formulating effective boundary conditions at the junction following the method suggested by Volkov [23].

Let us suppose that the size of the junction L_T exceeds the coherence length, $L_T \gg \xi_0$, and, simultaneously, does not exceed the Josephson penetration depth. Then the function \check{G} in the left-hand side (lhs) of the kinetic equation $[\check{H}, \circ \check{G}] = i\mathcal{D}\nabla\check{J}$ is approximately constant within the junction banks (parts of the junction leads of lengths L_T beneath and above the insulator). Then, integrating this equation over the volume of the bottom bank, using the

boundary conditions (5) and denoting the cross-section area of the lead as S_ℓ , the lead thickness as d , and the area of the junction as S_T , we obtain

$$\begin{aligned} S_T d [\check{H}, \circ \check{G}] &= i\mathcal{D} \{ S_T (W/\xi_0) [\check{G}_{-0}, \circ \check{G}_{+0}] - S_\ell \check{J}_\ell \}, \text{ or} \\ [\check{H}, \circ \check{G}] &= 2i\Delta \{ \tilde{W} [\check{G}_{-0}, \circ \check{G}_{+0}] - (\xi_0^2/L_T) \check{J}_\ell \}, \end{aligned} \quad (27)$$

where ± 0 denotes top and bottom side of the barrier, \check{J}_ℓ is the value of the matrix current at the lead cross-section adjoining the junction, and the tunnelling parameter \tilde{W} is defined as

$$\tilde{W} = W(\xi_0/d) = (3\xi_0^2/4\ell d)D. \quad (28)$$

As soon as $\xi_0 \ll L_T$ and $\xi_0 \check{J}_\ell \sim W$, the last term in (27) can be assumed to be the smallest one and thus neglected. However, this is only true for the Green's component of (27) [23],

$$[\check{H}, \circ \check{g}] = 2i\Delta \tilde{W} [\check{g}_{-0}, \circ \check{g}_{+0}], \quad (29)$$

whereas for the Keldysh component, the diagonal part of the lhs of (27) turns to zero (we consider only zero harmonics), and therefore the boundary condition for the diagonal part of \check{J}_ℓ^K , which is proportional to $D_+ \partial_x f$, has the form

$$\check{J}_\ell^K = (W_f/\xi_0) [\check{G}_{-0}, \circ \check{G}_{+0}]^K, \quad W_f = W(L_T/d) \gg \tilde{W}. \quad (30)$$

Equation (30) is the boundary condition for the distribution function, which is to be used as described in previous section. Solving the kinetic equation within the lead and assuming $L \gg L_T$, we arrive at the equation similar to (24) with the same parameter of nonequilibrium,

$$r = \frac{2W_f L}{\xi_0} = 2L \frac{R(\xi_0)}{2\xi_0 R} \frac{L_T}{d} = L \frac{\rho}{S_T R} \frac{L_T}{d} = \frac{L\rho}{S_\ell R} = \frac{R_N}{R},$$

where ρ is the specific conductivity of the leads.

5. Perturbation theory for the Green's functions

To calculate the DOS within the next approximation with respect to the parameter W , we solve the Usadel equation for the Green's function \hat{g} following from (7). Introducing usual parametrization $\hat{g} = \sigma_z \exp(\sigma_x \theta)$ and the dimensionless coordinate z , we arrive at the equation for the spectral angle θ ,

$$\sinh[\theta(z) - \theta_S] = i\theta''(z) \sinh \theta_S, \quad z = x/\xi_0 \quad (31)$$

(the prime sign denotes the derivative over z). With exponential accuracy, the solution of (31) at $z < 0$ can be approximated by the formula for a semi-infinite superconducting wire [30]

$$\tanh[(\theta(z) - \theta_S)/4] = \tanh[(\theta(-0) - \theta_S)/4] \exp(kz), \quad (32)$$

where $k^{-1}(E) = \sqrt{i \sinh \theta_S}$. Equation (32) describes the decay of perturbations of the spectral functions at distances $\gtrsim \xi_0$ from the barrier, where the spectral angle approaches its bulk value $\theta_S = \text{arctanh}(\Delta/E)$. The boundary condition for the spectral angle follows from (9a),

$$\theta' + W \sinh \theta (\cosh \theta_1 + \cosh \theta_{-1}) \Big|_{z=-0} = 0. \quad (33)$$

Then the boundary value of θ can be found from the finite-difference equation following from (33) and (32),

$$2k \sinh[(\theta_S - \theta)/2] = W \sinh \theta (\cosh \theta_1 + \cosh \theta_{-1}). \quad (34)$$

A similar result for the spectral angle in planar junction banks follows from (29),

$$k^2 \sinh(\theta_S - \theta) = \tilde{W} \sinh \theta (\cosh \theta_1 + \cosh \theta_{-1}). \quad (35)$$

In what follows, we will simultaneously discuss both of the junction geometries, using common notation W for both transparency parameters W and \tilde{W} and assuming this quantity to be defined by (10) or (28) depending on context.

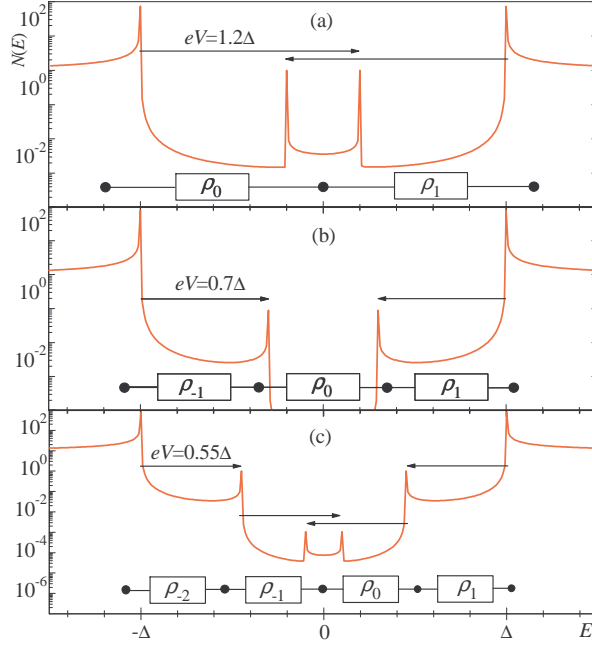


Figure 3. Numerically computed DOS and typical subgap circuits describing the two-particle current at $eV = 1.2\Delta$ (a), the three-particle current at $eV = 0.7\Delta$ (b), and the four-particle current at $eV = 0.55\Delta$ (c), for the tunnelling parameter $W = 10^{-3}$.

5.1. Simple perturbation theory

Due to the presence of the small parameter W in the right-hand side (rhs) of (34), one can suggest the following perturbation correction for θ to first order in W ,

$$\theta = \theta_S - Wk^{-1} \sinh \theta_S (\cosh \theta_{S,1} + \cosh \theta_{S,-1}), \quad (36)$$

and similar for (35). This results in the following expression for the DOS within the BCS gap,

$$N(E) = \text{Re}(\cosh \theta) = W|\Delta/\xi|^a (N_{S,1} + N_{S,-1}), \quad (37)$$

$$|\xi| = \sqrt{\Delta^2 - E^2}, \quad a = \begin{cases} 5/2, & \text{1D junction;} \\ 3, & \text{planar junction.} \end{cases}$$

Such approximation will be referred to as the result of a simple perturbation theory (SPT).

As follows from (37), the tunnelling coupling extends the DOS inside the gap over the distance eV from the gap edges, and scales it down by the factor W , as shown in figure 3. It is clear from (37) that with decreasing voltage, at $eV < \Delta$, the gap will open in the DOS (see figure 3(b)), and further iteration of the finite-difference equations (34) or (35) for the spectral angle is required. As the result of this iterative scheme, the DOS at small enough eV acquires a staircase structure in the energy space: two ladders descending from the bulk gap edges inside the subgap region; the height of n th step is W^n , and the width is eV . In the middle of the gap, $|E| < \Delta - (n-1)eV$ (assuming $eV < 2\Delta/n$), there is a plateau with the height $\approx 2W^n$ (see figures 3(a) and 3(c)). While eV decreases, the plateau expands until its size becomes equal to $2eV$, then a new pair of steps emerges, which happens when n is even. We recall that this deformation of the DOS occurs only locally, at the distance $x \sim \xi_0$ from the junction.

5.2. Improved perturbation theory

The subgap DOS in (37) possesses singularities at the gap edges $|E| = \Delta$, which causes a divergence of the subgap current at relatively large voltage, as we will see later. To eliminate the divergence, we need to apply an improved perturbation theory (IPT) to (34) and (35), in which nonlinearity of the recurrence relations is fully taken into account. First, we consider an approximation to (34), in which the non-singular terms $\cosh \theta_{\pm 1}$ are replaced with their BCS values, but we do not suppose that the difference $\theta - \theta_S$ is small,

$$\begin{aligned} \sinh[(\theta_S - \theta)/2] &= Wk^{-1} g(E, eV) \sinh \theta, \\ g(E, eV) &= \frac{1}{2} (\cosh \theta_{S,1} + \cosh \theta_{S,-1}). \end{aligned} \quad (38)$$

In the vicinity of the point $E = \Delta$ the function $g(E, eV)$ is regular and thus can be approximated by $g(\Delta, eV)$ (it is sufficient to consider only positive values of E due to the symmetry of the spectral functions). Within the region $|E - \Delta| \ll \Delta$, the spectral angles θ and θ_S are large, therefore we hold only large exponents $\exp \theta$ and $\exp \theta_S$ in the hyperbolic functions in the rhs of (38), and use the asymptotic expression $\exp \theta_S \approx [2\Delta/(E - \Delta)]^{1/2}$. Then, introducing a dimensionless energy variable ε and a normalized spectral function $z(\varepsilon)$,

$$\begin{aligned} \varepsilon &= (\Delta - E)/2\Delta p^2, & p(eV) &= [\frac{1}{2}W^2 g^2(eV)]^{1/3}, \\ z(\varepsilon) &= ip \exp \theta, & \exp \theta_S &= (ip\sqrt{\varepsilon})^{-1} \end{aligned} \quad (39)$$

we reduce (38) to a numerical algebraic equation

$$z^3 + (z\sqrt{\varepsilon} - 1)^2 = 0. \quad (40)$$

The relevant solution $z(\varepsilon)$ of (40) is determined by the requirement for the asymptotic behaviour at $\varepsilon \gg 1$ to coincide with the energy dependence $z(\varepsilon) \approx \varepsilon^{-1/2} + i\varepsilon^{-5/4}$ given by the direct perturbative expansion (36). For planar geometry, we directly obtain the function $z(\varepsilon)$ and the scaling parameter p from (35),

$$z(\varepsilon) = (\varepsilon - i)^{-1/2}, \quad p(eV) = [Wg(eV)]^{1/2}. \quad (41)$$

The resulting DOS in the region $|E - \Delta| \ll \Delta$,

$$N(E, eV) = [2p(eV)]^{-1} \text{Im } z(\varepsilon), \quad (42)$$

approaches a finite value $N(\Delta, eV) \sim W^{-b}(eV - 2\Delta)^{-b/2}$ at $E = \Delta$, where

$$b = \begin{cases} 2/3, & \text{1D junction;} \\ 1/2, & \text{planar junction.} \end{cases} \quad (43)$$

However, in the vicinity of the specific voltage value $eV = 2\Delta$ the DOS diverges, and the calculation procedure must be further improved. The problem is caused by the fact that at $eV = 2\Delta$ both the energies E and $E - eV$ in (34) or (35) approach the gap edges Δ and $-\Delta$, respectively. Therefore one must solve the equation not only for $N(E)$, but for $N(E - eV)$ as well. To this end we consider the recurrence (34) for these two energies and replace the nonsingular terms $\cosh \theta_1$ and $\cosh \theta_{-2}$ by their BCS values,

$$\begin{aligned} \sinh \frac{\theta_S - \theta}{2} &= \frac{W \sinh \theta}{2k} (\cosh \theta_{-1} + \cosh \theta_{S,1}), \\ \sinh \frac{\theta_{S,-1} - \theta_{-1}}{2} &= \frac{W \sinh \theta_{-1}}{2k_{-1}} (\cosh \theta_{S,-2} + \cosh \theta). \end{aligned} \quad (44)$$

Using again the fact that the spectral angles are large by modulus in the region $|E - \Delta| \ll \Delta$, we hold only large exponents $\exp \theta$, $\exp \theta_S \approx [2\Delta/(E - \Delta)]^{1/2}$ and $\exp(-\theta_{-1})$, $\exp(-\theta_{S,-1}) \approx [2\Delta/(eV - \Delta - E)]^{1/2}$ in the rhs of (44). Then, introducing dimensionless energy and voltage variables ε and Ω , and normalized spectral functions $z(\varepsilon)$ and $\bar{z}(\varepsilon)$,

$$\begin{aligned} \varepsilon &= (E - \Delta)/2\Delta q^2, & \Omega &= (eV - 2\Delta)/2\Delta q^2, \\ \exp \theta &= zq^{-1}, & \exp(-\theta_{-1}) &= \bar{z}q^{-1}, & q &= W^{2/5}/2. \end{aligned} \quad (45)$$

we obtain algebraic equations for the functions $z(\varepsilon)$ and $\bar{z}(\varepsilon)$, which reduce to a single equation for the function $z(\varepsilon)$,

$$[z^3(1 - zR)^{-2} + i\bar{R}^2]^2 + iz[(1 - zR)^2 - 4z\bar{R}] = 0, \quad (46)$$

where $R(\varepsilon) = \sqrt{\varepsilon + i0}$ and $\bar{R}(\varepsilon) = R(\Omega - \varepsilon)$. The function \bar{z} can be then found as $\bar{z} = (1 - zR)/\sqrt{iz^3}$. For planar geometry, we obtain the equations

$$(1 - z^2 R^2)^2 (z + i\bar{R}^2) + iz^4 = 0, \quad \bar{z} = (1 - z^2 R^2)/iz^2, \quad (47)$$

and the scaling parameter $q = (W/4)^{1/3}$. According to the definition of $z(\varepsilon)$ in (45), the solutions of (46) and (47) are related to the boundary values of the DOS as

$$N(E) = (2q)^{-1} \text{Re } z, \quad N_{-1}(E) = (2q)^{-1} \text{Re } \bar{z}. \quad (48)$$

The results of computation of the DOS based on the numerical solution of the recurrences (34) and (35) and shown in figure 3, quantitatively confirm the results of our asymptotic analysis.

6. Multiparticle currents: thresholds

6.1. Two-particle current

The existence of the subgap states enables quasiparticles to overcome the energy gap at $eV < 2\Delta$ via two steps involving intermediate Andreev reflection at the energy $|E| < \Delta$. The population $n(E)$ of the intermediate state is generally non-equilibrium, because the subgap quasiparticles cannot access the equilibrium electrodes. In terms of the circuit approach, the node $k = 0$ is disconnected from the equilibrium source, and the subgap current flows through two resistances ρ_0 and ρ_1 (two-particle current), see figure 3(a). The corresponding partial currents are equal, $j_0 = j_1 = [n_F(E_1) - n_F(E_{-1})]/(\rho_0 + \rho_1)$, and their contribution to $I(V)$ is confined to the energy region $0 < E < eV - \Delta$ (a similar contribution at $\Delta < E < eV$ comes from j_0 and j_{-1}), which leads to the following expression for the two-particle current,

$$I_2 = \frac{4}{eR} \int_0^{eV-\Delta} \frac{dE}{\rho_0 + \rho_1}, \quad \Delta \leq eV < 2\Delta.$$

Within the SPT approximation for the subgap DOS function N , this is equivalent to equation

$$I_2 = \frac{4W}{eR} \int_0^{eV-\Delta} dE \left| \frac{\Delta}{\xi} \right|^a \frac{|E_1 E_{-1}|}{\xi_1 \xi_{-1}}, \quad (49)$$

where $\xi(E) = [(E + i0)^2 - \Delta^2]^{1/2}$ according to (11b). The current I_2 increases with voltage and diverges at $eV = 2\Delta$ which is the result of the mentioned DOS singularity at $E = \Delta$.

At $eV = \Delta$, the two-particle current possesses a threshold. In the vicinity of the threshold, $eV = \Delta + \Omega$, $0 < \Omega \ll \Delta$, equation (49) simplifies, giving the current threshold value

$$I_2(\Delta) = \frac{2W\Delta}{eR} \int_0^\Omega \frac{dE}{\sqrt{\Omega^2 - E^2}} = \frac{\pi W\Delta}{eR} = 2WI_1(2\Delta). \quad (50)$$

6.2. Three-particle current

At $eV < \Delta$, a minigap opens in the DOS around the zero energy (see figure 3(b)), however, since the number of subgap resistors increases up to three: ρ_{-1} , ρ_0 and ρ_1 (three-particle current), the current across the minigap will persist as long as the network period exceeds the minigap size, $eV > 2(\Delta - eV)$, i.e., at $eV > 2\Delta/3$. The corresponding partial currents are equal, $j_{-1} = j_0 = j_1 = [n_F(E_1) - n_F(E_{-2})]/(\rho_{-1} + \rho_0 + \rho_1)$, and their contribution to $I(V)$ is confined to the energy region $\Delta - eV < E < 2eV - \Delta$, which leads to the following expression for the three-particle current at zero temperature,

$$I_3 = \frac{3}{eR} \int_{\Delta-eV}^{2eV-\Delta} \frac{dE}{\rho_{-1} + \rho_0 + \rho_1}, \quad 2\Delta/3 \leq eV < \Delta. \quad (51)$$

Taking the subgap DOS functions N and N_{-1} in the SPT approximation (37), we see that the central resistance $\rho_0 \sim W^{-2}$ is the largest. Retaining only this resistance, we get

$$I_3 = \frac{3W^2}{eR} \int_{\Delta-eV}^{2eV-\Delta} dE \left| \frac{\Delta^2}{\xi \xi_{-1}} \right|^a \frac{|E_1 E_{-2}|}{\xi_1 \xi_{-2}}. \quad (52)$$

While approaching the voltage value $eV = \Delta$, the current I_3 infinitely increases due to decreasing distance between the upper integration limit and the singular point $E = \Delta$. Calculating (52) in the vicinity of the threshold $eV = 2\Delta/3$, we obtain

$$I_3(2\Delta/3) = \frac{3\pi\Delta W^2}{2eR} \left(\frac{9}{8}\right)^a \approx 2WI_2(\Delta). \quad (53)$$

6.3. Four-particle current

At $eV < 2\Delta/3$ the network period becomes smaller than the minigap, and the situation resembles the one encountered when the voltage decreased below 2Δ : we have to calculate the next correction to the DOS $\sim W^2$. In the equation for the four-particle current,

$$I_4 = \frac{8}{eR} \int_0^{2eV-\Delta} \frac{dE}{\rho_{-1} + \rho_0 + \rho_1 + \rho_2}, \quad \frac{\Delta}{2} \leq eV < \frac{2\Delta}{3} \quad (54)$$

(see figure 3(c)), the largest resistances are $\rho_0 \sim \rho_1 \sim W^{-3}$, thus $\rho_{-1} \sim \rho_{-2} \sim W^{-1}$ can be neglected. The functions $N_{\pm 1}$ can be obtained from the SPT equations (37) at $E = E_{\pm 1}$, in which small N in the rhs has to be neglected:

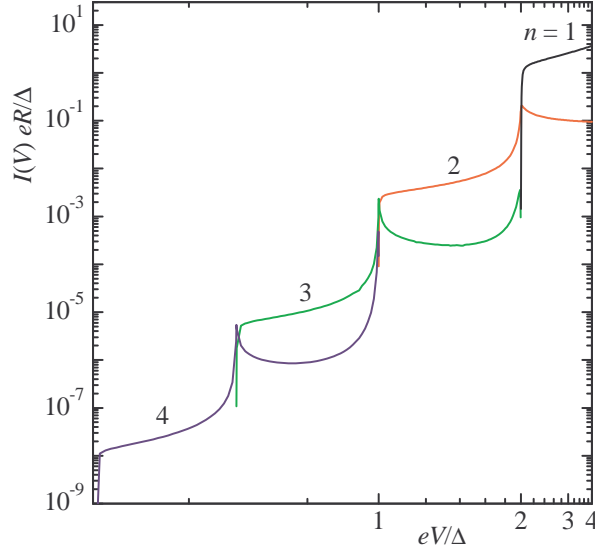


Figure 4. Multiparticle currents in planar junction numerically computed for the tunnelling parameter $W = 10^{-3}$.

$N_{\pm 1} = W|\Delta/\xi_{\pm 1}|^a N_{S,\pm 2}$. To evaluate the function N , we must perform next iteration step, by substituting these values of $N_{\pm 1}$ into the SPT equation (37) for N . As the result, we obtain

$$I_4 = \frac{8W^3}{eR} \int_0^{2eV-\Delta} dE \left| \frac{\Delta^3}{\xi \xi_{-1} \xi_1} \right|^a \frac{|E_2 E_{-2}|}{\xi_2 \xi_{-2}}.$$

While approaching the voltage value $eV = 2\Delta/3$, the current I_4 infinitely increases. In the vicinity of the threshold $eV = \Delta/2$ we have

$$I_4(\Delta/2) = \frac{2\pi\Delta W^3}{eR} \left(\frac{4}{3}\right)^a \approx 2WI_3(2\Delta/3). \quad (55)$$

From these considerations we conclude that the evaluation of $2n$ - and $(2n+1)$ -particle currents requires DOS recurrences of n th order. As long as the applied voltage decreases below Δ/n , a new minigap opens in the DOS (see discussion in section 5.1), and the recurrent procedure should be repeated again.

7. Multiparticle currents: large voltage

It follows from the previous section that the multiparticle currents calculated within the SPT approach have finite values in the vicinity of their thresholds, but they diverge at the next gap subharmonics: the two-particle current diverges at $eV = 2\Delta$, the three-particle current diverges at $eV = \Delta$, and so on. These divergences are caused by singularity of the SPT correction to the tunnelling DOS at the point $E = \Delta$ which enters the integration region.

It is easy to see that the two-particle current persists also above the gap voltage, $eV > 2\Delta$: when the node n_0 is inside the gap, $|E| < \Delta$, the subgap circuit should consist of two resistors no matter how large the applied voltage is. Furthermore, since the singular point $E = \Delta$ always belongs to the integration region, the current will formally diverge at *all voltages* $eV > 2\Delta$; generally, the n -particle current ($n > 1$) taken in the SPT approximation diverges at all voltages above $eV = 2\Delta/(n-1)$. This catastrophe is known since the pioneering calculations of the two-particle current within the tunnelling Hamiltonian model [1] but it can be eliminated by using the improved perturbation expansion of section 5.2. This implies in fact that the currents have nonanalytical dependencies on the tunnelling parameter W at large voltages.

We also note that the three-particle current disappears at large enough voltage, in contrast to the two-particle current which persists at all voltages above Δ/e . This is obvious from the circuit geometry in figure 3: as soon as eV exceeds 2Δ , the network period becomes larger than the energy gap, therefore the subgap circuit may involve no more than two resistors. This is relevant for all n -particle currents with $n > 2$ which persist only within the voltage intervals $2\Delta/n < eV < 2\Delta/(n-2)$ and abruptly disappear at larger voltages (see figure 4).

7.1. Two-particle current at $eV \geq 2\Delta$

The two-particle current at $eV > 2\Delta$ is given by equation

$$I_2 = \frac{4}{eR} \int_0^\Delta \frac{dE}{\rho_0 + \rho_1} = \frac{4}{eR} \int_0^\Delta dE \frac{NN_1 N_{-1}}{N_1 + N_{-1}}. \quad (56)$$

To evaluate the integral, we use the IPT equations (39)–(42) to calculate N , while the functions $N_{\pm 1}$ are taken in the BCS form. Furthermore all the smooth functions can be approximated with their values at the singular point $E = \Delta$,

$$g(eV) = \frac{1}{2} \sum_{k=\pm 1} N_S(\Delta + keV), \quad (57a)$$

$$N_1^{-1} + N_{-1}^{-1} = \sum_{k=\pm 1} N_S^{-1}(\Delta + keV) \equiv h^{-1}(eV). \quad (57b)$$

As it was expected, the two-particle current in this region is given by a nonanalytical expression with respect to W , and it is larger than the current value at smaller voltages $eV < \Delta$,

$$I_2 = \frac{2\Delta}{eR} C_1 p(eV) h(eV) \sim W^b, \quad (58)$$

$$C_1 = \int_0^\infty d\varepsilon \operatorname{Im} z(\varepsilon) = \begin{cases} 9\sqrt{3}/4, & \text{1D junction,} \\ \sqrt{2}, & \text{planar junction.} \end{cases}$$

Here $p(eV)$ is given by (39) or (41) depending on the junction geometry.

Important property of the tunnelling IVC is the excess current I_{exc} , i.e., voltage-independent deviation of the total current from the ohmic IVC at large voltage $eV \gg \Delta$. The excess current is readily evaluated by considering this limit in (7.1) and (58),

$$I_{\text{exc}} = \frac{\Delta}{eR} W^b \times \begin{cases} 6.19, & \text{1D junction,} \\ 2.83, & \text{planar junction.} \end{cases} \quad (59)$$

Our analysis is not complete yet because the current in (58) grows infinitely when the voltage approaches 2Δ . This divergence, caused by the singularity of N_{-1} in (57a), can be eliminated by using a more accurate approximation (45)–(48) for N . Neglecting a nonsingular term N_1 in the denominator in (56) and approximating N_1 with $N(3\Delta) = 3/2\sqrt{2}$, we obtain

$$\begin{aligned} I_2(2\Delta) &\approx \frac{4}{eR} \int_0^\Delta dE NN_1 = \frac{6q\Delta}{\sqrt{2}eR} \int_0^\infty d\varepsilon \operatorname{Re} z(-\varepsilon) \\ &\approx \frac{\Delta}{eR} W^{1/a} \times \begin{cases} 2.32, & \text{1D junction,} \\ 2.50, & \text{planar junction.} \end{cases} \end{aligned} \quad (60)$$

Thus we see that the two-particle current possesses a pronounced peak at $eV = 2\Delta$, which exceeds not only the current threshold value, but also the large excess current, see figure 4.

7.2. Three-particle current at $eV \geq \Delta$

The three-particle current at $eV \geq \Delta$ is given by (51), in which the integration interval is now $eV - \Delta < E < \Delta$. Using the symmetry relation $N(E) = N(-E)$, we reduce the integration region to the interval $eV/2 < E < \Delta$, containing only one dangerous point $E = \Delta$,

$$I_3 = \frac{6}{eR} \int_{eV/2}^\Delta \frac{dE}{\rho_{-1} + \rho_0 + \rho_1}. \quad (61)$$

At this point, all terms in the denominator turn to zero being calculated within the SPT approximation. To eliminate the divergence, we apply the IPT approach, (42) and (39), to calculate N , which then acquires a finite value $\sim W^{-b}$ at the singular point. In the present case the function g defined in (38) has a complex-valued form $g(eV) = |g|e^{i\varphi}$ because the energy E_{-1} in this equation occurs inside the gap,

$$|g| = \frac{\Delta^{3/2}}{\sqrt{eV[(2\Delta)^2 - (eV)^2]}}, \quad \tan \varphi = \frac{eV - \Delta}{eV + \Delta} \sqrt{\frac{2\Delta + eV}{2\Delta - eV}}. \quad (62)$$

Thus the scaling factor p in (39), (41) and (42) is to be defined through the modulus of g , while the phase factor will remain in the equation for z in the 1D geometry,

$$z^3 \exp(2i\varphi) + (z\sqrt{\varepsilon} - 1)^2 = 0, \quad (63)$$

and in the expression for z in planar geometry,

$$z = [\varepsilon - i \exp(i\varphi)]^{-1/2}. \quad (64)$$

Therefore the normalized spectral function becomes dependent on eV . The function N_{-1} can then be evaluated from the SPT approximation, keeping only large quantity N in the rhs,

$$N_{-1} = W |\Delta / \xi_{-1}|^a N. \quad (65)$$

At the singular point, $N_{-1} \sim W^{1-b}$; the other relevant functions N_1 and N_{-2} can be taken in the BCS form. Retaining only the largest resistance $\rho_{-1} \sim W^{b-1}$ in (61), we get

$$I_3 = \frac{6}{eR} \int_{eV/2}^{\Delta} dE N_{-1} N_{-2} = \frac{6Wp\Delta}{eR} N_{-2} \left| \frac{\Delta}{\xi_{-1}} \right|^a C_2 \sim W^{1+b},$$

$$C_2(eV) = \int_0^{\infty} d\varepsilon \operatorname{Im} z(\varepsilon, eV) \quad (66)$$

(for the planar model, $C_2(eV) = 2\cos(\varphi/2 + \pi/4)$). Here the functions N_{-2} and ξ_{-1} should be taken at the point $E = \Delta$. This expression diverges at $eV = \Delta$ and $eV = 2\Delta$. In fact, the current has a finite peak value at $eV = \Delta$; another peak appears slightly below $eV = 2\Delta$, because the current turns to zero at $eV = 2\Delta$, as follows from (61) (see figure 4).

At $eV = \Delta$, the function N_{-2} is also large at the point $E = \Delta$ and should be kept in (65) together with N , i.e., $N_{-1} = W(N + N_{-2})$; both these functions are to be evaluated using the IPT scheme (38)–(42). This leads to expressions $N = (2p)^{-1} \operatorname{Im} z_+(\varepsilon)$ and $N_{-2} = (2p)^{-1} \operatorname{Re} z_-(\varepsilon)$, where the functions z_{\pm} are given by the solutions of algebraic equations

$$z_+^3 + (z_+ \sqrt{\varepsilon} - 1)^2 = 0, \quad iz_-^3 + (z_- \sqrt{\varepsilon} - 1)^2 = 0 \quad (67)$$

in the case of 1D junction, or by explicit expressions

$$z_{\pm} = (\varepsilon \mp i)^{-1/2} \quad (68)$$

for a planar junction; the scaling parameter p is $(W^2/6)^{1/3}$ and $(W/\sqrt{3})^{1/2}$, respectively. Then the largest resistances are $\rho_0 \sim \rho_{-1} \sim W^{2b-1}$, and we obtain

$$I_3(\Delta) = \frac{6W}{eR} \int_{\Delta/2}^{\Delta} dE N N_{-2} = \frac{3W\Delta}{eR} \int_0^{\infty} d\varepsilon \operatorname{Im} z_+ \operatorname{Re} z_-$$

$$= \frac{W\Delta}{eR} \times \begin{cases} 3.16, & \text{1D junction;} \\ 3\pi/4, & \text{planar junction.} \end{cases} \quad (69)$$

Analysis of the current behaviour near $eV = 2\Delta$, which we do not present here, gives the following estimate for the current peak value: $I_{3\max} \sim W^{4/5} \Delta / eR$ for the 1D junction and $I_{3\max} \sim W\Delta / eR$ for the planar junction.

7.3. Four-particle current at $eV \geq 2\Delta/3$

The four-particle current at $eV \geq 2\Delta/3$ is given by (54), where the upper integration limit is replaced by the value $\Delta - eV$, representing a singular point of the integrand. The functions N and N_{-1} are calculated from the SPT equations (37), neglecting their values in the rhs,

$$N = W |\Delta / \xi|^a N_1, \quad N_{-1} = W |\Delta / \xi_{-1}|^a N_{-2}. \quad (70)$$

Within the voltage interval $2\Delta/3 < eV < \Delta$ we can apply the BCS approximation for the functions $N_{\pm 2}$. However, the function N_1 must be calculated by means of the IPT (38)–(42), as soon as the energy E_1 hits the singular point. The resulting equations for N_1 coincide with (62)–(64) for N in the previous section. Thus, at the singular point, $N_1 \sim W^{-b}$, $N_0 \sim W^{1-b}$, $N_{-1} \sim W$, and $N_{\pm 2} \sim 1$. Therefore the resistance $\rho_0 \sim W^{b-2}$ dominates, which gives

$$I_4 = \frac{8\Delta W^2}{eR} C_2(eV) p(eV) \left| \frac{\Delta^2}{\xi \xi_{-1}} \right|^a N_{-2} \sim W^{2+b}, \quad (71)$$

where the functions ξ , ξ_{-1} , and N_{-2} are taken at $E = \Delta - eV$. This expression diverges at the points $eV = 2\Delta/3$ and $eV = \Delta$, where the IPT should be applied. Since the SPT approximation for N_{-2} diverges at $eV = 2\Delta/3$, we evaluate both the functions N_1 and N_{-2} in the rhs of (70) using the IPT equations (38)–(42),

$$N_1(E) = (2p)^{-1} \operatorname{Im} z_+(\varepsilon), \quad N_{-2}(E) = (2p)^{-1} \operatorname{Re} z_-(\varepsilon). \quad (72)$$

The functions z_{\pm} obey the equations (67) or (68) modified by the phase factors similar to (63) and (64). In this case, $\tan \varphi = -\sqrt{2}/5$, and the scaling factor is $p = \frac{3}{4}(W^2/2)^{1/3}$ for 1D junctions and $p = (3W\sqrt{3}/8)^{1/2}$ for planar junctions. The corresponding estimates for the DOS functions are $N_1 \sim N_{-2} \sim W^{-b}$, $N \sim N_{-1} \sim W^{1-b}$, while $N_2 \sim 1$ can still be taken in the BCS approximation. Therefore the largest resistance is $\rho_0 \sim W^{2b-2}$, and we get

$$\begin{aligned} I_4(2\Delta/3) &= \frac{4\Delta W^2}{eR} \left(\frac{9}{8}\right)^a \int_0^\infty d\varepsilon \operatorname{Im} z_+ \operatorname{Re} z_- \\ &= \frac{\Delta W^2}{eR} \times \begin{cases} 6.63, & \text{1D junction;} \\ 5.26, & \text{planar junction.} \end{cases} \end{aligned} \quad (73)$$

Analysis of the current peak near $eV = \Delta$ gives the estimate $I_{4\max} \sim W\Delta/eR$.

8. Effect of first harmonics

In this Section we evaluate the effect of higher harmonics on the dc subgap current. We restrict our calculation to first order in the tunnelling parameter W thus taking into account only two first harmonics $m = \pm 1$. The main conclusion of our calculation will be that including harmonics produces just insignificant quantitative changes, while major qualitative properties of the SGS, positions and scaling of the current steps will not change. We start with a general equation (14) for the dc current, and evaluate an additional contribution due to the first harmonics of the boundary values of the Keldysh and Green's functions,

$$\begin{aligned} \delta I &= \int_{-\infty}^{\infty} \frac{dE}{32eR} \operatorname{Tr} \sum_{m=\pm 1} m \sigma_z [\hat{h}(E, 0) \hat{G}^K(E, m) \\ &\quad + \hat{h}(E, -m) \hat{G}^K(E, 0)] \\ &= i \int_{-\infty}^{\infty} \frac{dE}{4eR} \sum_{m=\pm 1} m [V_y(E, m) \operatorname{Im} v + V \operatorname{Im} v_y(E, m)]. \end{aligned} \quad (74)$$

Here and below we use the subscripts (x, y, z) to indicate the matrix components of the first harmonics of the Green's and Keldysh functions, while the zero harmonics will be used as before without such subscripts. Thus v [V] in (74) indicates y -component of $\hat{g}(E, 0)$ [$\hat{G}^K(E, 0)$], and $v_y(E, \pm 1)$ [$V_y(E, \pm 1)$] indicates the y -component of $\hat{g}(E, \pm 1)$ [$\hat{G}^K(E, \pm 1)$].

8.1. Perturbation theory for the Green's functions

To evaluate the current in (74), one needs to find the y -component in the Green's function expansion over the Pauli matrices, $\hat{g}(z, E, m) = \sigma_z u_z + i\sigma_y v_y + \sigma_x v_x + w$. In what follows, we will focus on the case of 1D junction. Considering the Usadel equation (7) to first order in W , we arrive at the equation for the functions $v_y(z, E, m)$ and $u_z(z, E, m)$,

$$meV u_z = 2i\Delta (u_m u_z'' - v_m v_y''). \quad (75)$$

In this and following derivations we neglect small deviation of the functions u and v from the BCS form (11b). We use the following convention: the zero harmonics with shifted energy arguments $E + meV$ will be denoted with the subscript m , as before, e.g., $u_m \equiv u(E + meV, 0)$, while the first harmonics will be denoted with an argument, e.g., $v_y(E, \pm 1)$; the absence of the explicit argument would mean the relevance to the both harmonics $m = \pm 1$.

The function u_z can be excluded from (75) by virtue of the normalization condition $(u_1 + u_{-1})u_z = (v_1 + v_{-1})v_y$ following from (7). The boundary condition for (75) results from (9a) and determines the boundary value of first derivative,

$$v_y'|_{z=0} = (W/2)v(1 + u_1 u_{-1} + v_1 v_{-1}). \quad (76)$$

Solution of (75), $v_y(z) = v_y \exp(k_1 z)$ at $z < 0$, leads to the following relation at the boundary,

$$v_y(E, m) = k_1^{-1} v_y'(E, m), \quad k_1^2 = (\xi_1 + \xi_{-1})/2i\Delta. \quad (77)$$

Equations (76) and (77) allow us to express the first harmonics $v_y(E, m)$ through known zero harmonics u and v , and to establish the relation $v_y(E, 1) = v_y(E, -1)$ which implies that the second term in (74) turns to zero.

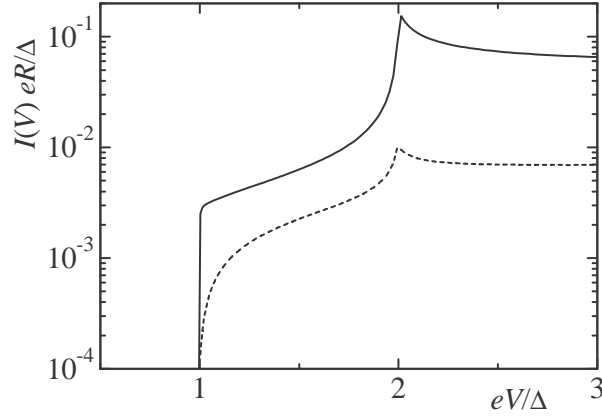


Figure 5. Current of first harmonics (dashed line) compared to the two-particle current (solid line), for the tunnelling parameter $W = 10^{-3}$.

8.2. Perturbation theory for Keldysh function

To calculate the harmonics of the Keldysh function, it is convenient to separate the contributions of the harmonics of the Green's function and the distribution function,

$$\begin{aligned}\hat{G}^K(E, m) &= \delta\hat{G}^K(E, m) + \hat{G}^K(E, m), \\ \delta\hat{G}^K(E, m) &= \hat{g}^R(E, m)f_{-m} - f_m\hat{g}^A(E, m), \\ \hat{G}^K(E, m) &= \hat{g}_m^R f(E, m) - f(E, m)\hat{g}_{-m}^A.\end{aligned}\tag{78}$$

In (78) we used the rule (12) for the convolutions valid for the first harmonics, $(A \circ B)(E, m) = A(E, m)B_{-m} + A_m B(E, m)$, which allows us to write the equation for the function \hat{G}^K following from (8a) and (9b) in a symbolic form

$$[\hat{H}, \circ \hat{G}^K] = 2i\Delta \partial_x (\hat{g}^R \circ \partial_x \hat{G}^K + \hat{G}^K \circ \partial_x \hat{g}^A),\tag{79}$$

where a small gradient of the distribution function, $\partial_x f \sim L^{-1}$, has been neglected. The boundary condition to (79) reads

$$\hat{g}^R \circ \partial_x \hat{G}^K = W (\hat{g}^R \circ \hat{\mathcal{F}} - \hat{\mathcal{F}} \circ \hat{g}^A),\tag{80}$$

where $\hat{\mathcal{F}} = \hat{g}^R \circ (\bar{f} - f) - (\bar{f} - f) \circ \hat{g}^A$. According to (74) and (78), we are interested in the y -component in the expansion $\hat{G}^K = \sigma_z \mathcal{U}_z + i\sigma_y \mathcal{V}_y + \sigma_x \mathcal{V}_x + \mathcal{W}$. Equation for this component, $meV\mathcal{U}_z = 2i\Delta (u_m \mathcal{U}_z'' - v_m \mathcal{V}_y'')$, follows from (79) and looks similar to (75). The normalization condition (8b) gives the relation $(v_m - v_{-m}^*)\mathcal{U}_z = (u_m - u_{-m}^*)\mathcal{V}_y$ which allows us to obtain a closed differential equation for \mathcal{V}_y . Solution $\mathcal{V}_y(z) = \mathcal{V}_y \exp(q_1 z)$ of this equation at $z < 0$ gives the following relation at the boundary,

$$\mathcal{V}_y(E, m) = q_1^{-1} \mathcal{V}_y'(E, m), \quad q_1^2 = (\xi_1 - \xi_{-1}^*)/2i\Delta,\tag{81}$$

where the quantity \mathcal{V}_y' is to be determined from the boundary condition (80),

$$\begin{aligned}\mathcal{V}_y'|_{z=0} &= W (1 - u_m u_{-m}^* - v_m v_{-m}^*) \Phi(E, m), \\ \Phi(E, m) &= M \left(f - \frac{1}{2} \sum_{k=\pm 1} f_k \right) + \frac{i}{2} M_S \operatorname{sgn}(m) \sum_{k=\pm 1} k f_k,\end{aligned}\tag{82}$$

where $M_S = \operatorname{Im} v$. At $T = 0$ we obtain $\Phi(E, m) = \Theta(eV - |E|)[M \operatorname{sgn}(E) + iM_S \operatorname{sgn}(m)]$.

8.3. Current of first harmonics

The function $V_y(E, m)$, which determines the current in (74), is now expressed, according to (78), through the quantities calculated in (76)–(77) and (81)–(82), $V_y(E, m) = v_y f_{-m} + v_y^* f_m + \mathcal{V}_y$. Collecting all these equations and substituting them into (74), we get

$$\begin{aligned}\delta I &= \frac{W}{4eR} \int_{-\infty}^{\infty} dE \operatorname{Im} v \{ (f_1 - f_{-1}) \operatorname{Im} (v k_1^{-1} \cosh^2 \chi) \\ &+ \operatorname{Im} [v q_1^{-1} (f - f_{-1}) + v^* q_1^{-1} (f - f_1) \sinh^2 \tilde{\chi}] \},\end{aligned}$$

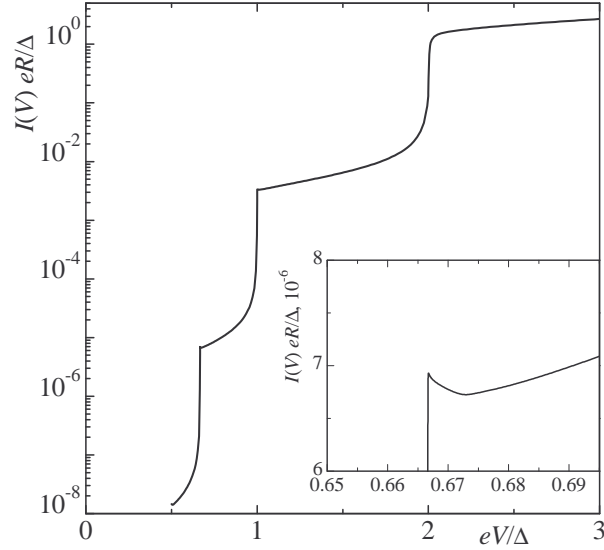


Figure 6. I - V characteristic with tunnelling SGS for planar junction computed numerically for the tunnelling parameter $W = 10^{-3}$. The inset shows a spike of the IVC near the threshold $eV = 2\Delta/3$ of the three-particle current.

Table 1. Threshold and peak values of the normalized multiparticle currents $I_n eR/\Delta$, $n = 1 \div 4$. The left and right sub-columns correspond to the 1D and planar models of the tunnel junction, respectively.

n	$eV = 2\Delta/n$		$eV = 2\Delta/(n-1)$		$eV = 2\Delta/(n-2)$	
1	$\pi/2$		—		—	
2	πW		$2.32W^{2/5}$	$2.50W^{1/3}$	$6.19W^{1/3}$	$2.83W^{1/2}$
3	$6.33W^2$	$6.71W^2$	$3.16W$	$2.36W$	$0.44W^{4/5}$	$3.57W$
4	$12.9W^3$	$14.9W^3$	$6.63W^2$	$5.26W^2$	$0.57W$	$0.48W$

where $\chi = \frac{1}{2}(\theta_1 + \theta_{-1})$ and $\tilde{\chi} = \frac{1}{2}(\theta_1 + \theta_{-1}^*)$. At $T = 0$, this equation simplifies:

$$\delta I = \frac{2W}{eR} \int_0^{eV} dE \operatorname{Im} v \operatorname{Im} [v(k_1^{-1} \cosh^2 \chi + q_1^{-1} \sinh^2 \tilde{\chi})]. \quad (83)$$

Similar considerations in the case of a planar junction result in replacements $q_1 \rightarrow q_1^2$ and $k_1 \rightarrow k_1^2$ in the rhs of (83). Noting that at $eV < \Delta$ the energy E_{-1} in (83) appears in the subgap region, where $\theta_{-1}^* = \theta_{-1} + i\pi$ and $\xi_{-1}^* = -\xi_{-1}$, we find that δI turns to zero at $eV < \Delta$, similar to I_2 . Numerical calculations show that the contribution of the first harmonics to the net dc current does not exceed 30% (see figure 5). From this we conclude that the adopted quasi-static approximation, where the nonzero harmonics are neglected, gives a relatively good approximation to a complete solution.

9. Discussion

Our analysis of the high-order multiparticle currents shows that they exhibit a similar pattern of the voltage dependence (see figure 4): an n -particle current appears above the threshold $eV = 2\Delta/n$, having roughly the value $I_n \sim (2W)^{n-1} I_1$, then increases and shows dramatic peak while approaching $eV = 2\Delta/(n-1)$; then it remains anomalously large within the voltage interval $2\Delta/(n-1) < eV < 2\Delta/(n-2)$ and eventually disappears at $eV = 2\Delta/(n-2)$, showing another strong peak at slightly smaller voltage. For convenience, all the threshold and peak values of the first four currents are brought together in the table 1.

The net tunnel current consists of the sum of the n -particle currents, and therefore exhibits a pronounced step-like structure on the IVC with steps at the gap subharmonics $eV = 2\Delta/n$, as shown in figure 6 obtained by numerical calculation at $T = 0$. The peaks of the multiparticle currents with numbers $n+1$ and $n+2$ produce small spikes at the n th threshold with $n > 1$; the example of such spike is presented in the inset of figure 6. The numerical procedure involves solving the set of recurrences (34) or (35) for the functions θ_k which correspond to the subgap energies, $|E_k| \leq \Delta$ ($-N_- < k < N_+$); the nonsingular terms in these equations are replaced with the BCS values. For the voltage values equal to the gap subharmonics one more equation is to be added as explained in the previous sections. We note that the results for the 1D and planar geometries differ insignificantly for equal

values of the tunnelling parameter (10) and (28); in logarithmic scale, the difference can be detected only in the immediate vicinity of the peaks.

Such a picture is quite similar to the tunnelling SGS in quantum point contacts [2, 3, 4, 11, 13], and the resulting IVC is found to be very close to the result for a point contact with the effective transparency $D_{\text{eff}} = 4W$. Thus, according to the definitions (10) and (28) of the tunnelling parameter W , the enhancement factor D_{eff}/D for the SGS scaling is equal to $3\xi_0/\ell$ in the 1D junction and $3\xi_0^2/d\ell$ in the planar junction. In particular, for planar Al junctions with $\ell \sim d = 50$ nm and $\xi_0 = 300$ nm, the enhancement factor may approach the value 100.

The fact that the SGS in planar junctions is sensitive to the properties of the junction electrodes has important implications for characterization of the junction tunnelling layer. Indeed, the thickness of this layer in realistic junctions is inhomogeneous: there are spots with enhanced transparency, which mostly contribute to the tunnel current. If the linear sizes of such spots are large compared to the electron mean free path in the electrodes (in practice, the thickness of thin-film electrodes), the junction can be considered as a quasi-planar one, and the SGS should be enhanced according to our theory and depend on the electrode thickness. However, if such spots are small compared to the electron mean free path, the tunnel current rapidly spreads out in immediate vicinity of the spot without being affected by the impurity scattering, as it is in the ballistic constrictions; in this case, there must be no dependence of the SGS on the electrode properties in accord with the mesoscopic theory prediction [2, 3, 4].

Acknowledgments

The support from the SSF-OXIDE Consortium, the Swedish Research Council (VR), and the Royal Academy of Science (KVA) is gratefully acknowledged.

References

- [1] Schrieffer J R and Wilkins J W 1963 *Phys. Rev. Lett.* **10** 17; Wilkins J W 1963 *Tunnelling Phenomena in Solids* (New York: Plenum) p 333; Hasselberg L E, Levinsen M T and Samuelsen M R 1974 *Phys. Rev. B* **9** 3757
- [2] Bratus' E N, Shumeiko V S and Wendin G 1995 *Phys. Rev. Lett.* **74** 2110
- [3] Cuevas J C, Martin-Rodero A and Yeyati A L 1996 *Phys. Rev. B* **54** 7366
- [4] Averin D and Bardas A 1995 *Phys. Rev. Lett.* **75** 1831
- [5] Arnold G B 1987 *J. Low Temp. Phys.* **68** 1
- [6] Klapwijk T M, Blonder G E and Tinkham M 1982 *Physica B+C* **109-110** 1657
- [7] Taylor B N and Burstein E 1963 *Phys. Rev. Lett.* **10** 14; Rowell J M 1964 *Rev. Mod. Phys.* **36** 215
- [8] Marcus S M 1966 *Phys. Lett.* **19** 623; Marcus S M 1966 *Phys. Lett.* **20** 236; Rowell J M and Feldmann W L 1968 *Phys. Rev. B* **172** 393
- [9] Foden C L, Rando N, van Dordrecht A, Peacock A, Lumley J and Pereira C 1993 *Phys. Rev. B* **47** 3316; Cristiano R, Frunzio L, Monaco R, Nappi C and Pagano S 1994 *Phys. Rev. B* **49** 429
- [10] Patel V and Lukens J E 1999 *IEEE Trans. Appl. Supercond.* **9** 3247; Gubrud M A, Ejtnaes M, Berckley A J, Ramos R C (Jr), Anderson J R, Dragt A J, Lobb C J and Wellstood F C 2001 *IEEE Trans. Appl. Supercond.* **11** 1002; Lang K M, Nam S, Aumentado J, Urbina C and Martinis J M 2003 *IEEE Trans. Appl. Supercond.* **13** 989; Oh S, Cical K, McDermott, Cooper K B, Osborn K D, Simmonds R W, Steffen M, Martinis J M and Pappas D P 2005 *Supercond. Sci. Technol.* **18**, 1396
- [11] van der Post N, Peters E T, Yanson I K and van Ruitenbeek J M 1994 *Phys. Rev. Lett.* **73** 2611.
- [12] Scheer E, Joyez P, Esteve D, Urbina C and Devoret M H 1997 *Phys. Rev. Lett.* **78** 3535
- [13] Ludoph B, van der Post N, Bratus' E N, Bezuglyi E V, Shumeiko V S, Wendin G and van Ruitenbeek J M 2000 *Phys. Rev. B* **61** 8561; Naaman O and Dynes R C 2004 *Solid State Commun.* **129** 299
- [14] Kleinsasser A W, Miller R E, Mallison W H and Arnold G B 1994 *Phys. Rev. Lett.* **72** 1738
- [15] Bezuglyi E V, Vasenko A S, Bratus' E N, Shumeiko V S and Wendin G 2006 *Phys. Rev. B* **73** 220506(R)
- [16] Larkin A I and Ovchinnikov Yu N 1986 *Nonequilibrium Superconductivity (Modern Problems in Condensed Matter Sciences vol 12)* ed D N Langenberg and A I Larkin (Amsterdam: North-Holland) p 493
- [17] Belzig W, Wilhelm F K, Bruder C, Schön G and Zaikin A D 1999 *Superlatt. Microstruct.* **25** 1251; Eschrig M 2000 *Phys. Rev. B* **61** 9061
- [18] Bezuglyi E V, Bratus' E N, Shumeiko V S, Wendin G and Takayanagi H 2000 *Phys. Rev. B* **62** 14439
- [19] Cuevas J C, Hammer J, Kopu J, Viljas J K and Eschrig M 2006 *Phys. Rev. B* **73** 184505; Bobkova I V and Bobkov A M 2006 *Phys. Rev. B* **74** 220504
- [20] Nazarov Yu V 1999 *Superlatt. Microstruct.* **25** 1221
- [21] Beenakker C W J 1991 *Phys. Rev. Lett.* **67** 3836; Beenakker C W J 1992 *Phys. Rev. Lett.* **68** 1442; Bardas A and Averin D 1997 *Phys. Rev. B* **56** R8518
- [22] Beenakker C W J, Rejai B and Melsen J A 1994 *Phys. Rev. Lett.* **72** 2470
- [23] Volkov A F 1994 *Physica B* **203** 267
- [24] Werthamer N R 1966 *Phys. Rev.* **147** 255; Larkin A I and Ovchinnikov Yu N 1967 *Sov. Phys.-JETP* **24** 1035
- [25] Kupriyanov M Yu 1992 *JETP Lett.* **56** 399; Bezuglyi E V, Bratus' E N and Galaiko V P 1999 *Low Temp. Phys.* **25** 167; Galaktionov A V and Chang-Mo Ryu 2000 *J. Phys.: Condens. Matter* **12** 1351.
- [26] Kupriyanov M Yu and Lukichev V F 1988 *Sov. Phys.-JETP* **67** 1163
- [27] Ovchinnikov Yu N 1971 *Sov. Phys.-JETP* **32** 72
- [28] Artemenko S N, Volkov A F and Zaitsev A V 1979 *Sov. Phys.-JETP* **49** 924
- [29] Bezuglyi E V, Vasenko A S, Shumeiko V S and Wendin G 2005 *Phys. Rev. B* **72** 014501.
- [30] Bezuglyi E V and Vinokur V 2003 *Phys. Rev. Lett.* **91** 137002.